



## ORIGINAL ARTICLE

# Prognostic value of lesion dissemination in doxorubicin, bleomycin, vinblastine, and dacarbazine-treated, interimPET-negative classical Hodgkin Lymphoma patients: A radio-genomic study

Rexhep Durmo<sup>1,2</sup> | Benedetta Donati<sup>3</sup> | Louis Rebaud<sup>4,5</sup> |  
Anne Segolene Cottureau<sup>6</sup> | Alessia Ruffini<sup>7</sup> | Maria Elena Nizzoli<sup>7</sup> |  
Sabino Ciavarella<sup>8</sup> | Maria Carmela Vegliante<sup>8</sup>  | Christophe Nioche<sup>4</sup> |  
Michel Meignan<sup>9</sup> | Francesco Merli<sup>7</sup> | Annibale Versari<sup>1</sup> | Alessia Ciarrocchi<sup>3</sup>  |  
Irene Buvat<sup>4</sup> | Stefano Luminari<sup>7,10</sup>

<sup>1</sup>Nuclear Medicine Unit, Azienda USL-IRCCS, Reggio Emilia, Italy

<sup>2</sup>PhD Program in Clinical and Experimental Medicine (CEM), University of Modena and Reggio Emilia, Modena, Italy

<sup>3</sup>Translational Research Laboratory, Azienda USL-IRCCS, Reggio Emilia, Italy

<sup>4</sup>Laboratoire d'Imagerie Translationnelle en Oncologie, Institut Curie, U1288 Inserm, PSL, Orsay, France

<sup>5</sup>Siemens Healthineers, Saint-Denis, France

<sup>6</sup>Department of Nuclear Medicine, Cochin Hospital, AP-HP, Université de Paris, Paris, France

<sup>7</sup>Hematology Unit, Azienda USL-IRCCS, Reggio Emilia, Italy

<sup>8</sup>Hematology and Cell Therapy Unit, IRCCS-Istituto Tumori 'Giovanni Paolo II', Bari, Italy

<sup>9</sup>Lysa Imaging, Henri Mondor University Hospital, AP-HP, University Paris East, Creteil, France

<sup>10</sup>Surgical, Medical and Dental Department of Morphological Sciences Related to Transplant, Oncology and Regenerative Medicine, University of Modena and Reggio Emilia, Reggio Emilia, Italy

## Correspondence

Stefano Luminari, Hematology Unit, Azienda USL-IRCCS di Reggio Emilia, Reggio Emilia, Italy.

Email: [Stefano.Luminari@ausl.re.it](mailto:Stefano.Luminari@ausl.re.it)

Alessia Ciarrocchi, Laboratory of Translational Research, Azienda USL-IRCCS di Reggio Emilia, Reggio Emilia, Italy.

Email: [Alessia.Ciarrocchi@ausl.re.it](mailto:Alessia.Ciarrocchi@ausl.re.it)

## Funding information

GRADE Onlus; Associazione Italiana per la Ricerca sul Cancro; Italian Ministry of Health – Ricerca Corrente Annual Program 2023 Open Access Funding provided by Università degli Studi di Modena e Reggio Emilia within the CRUI-CARE Agreement.

## Abstract

We evaluated the prognostic role of the largest distance between two lesions (Dmax), defined by positron emission tomography (PET) in a retrospective cohort of newly diagnosed classical Hodgkin Lymphoma (cHL) patients. We also explored the molecular bases underlying Dmax through a gene expression analysis of diagnostic biopsies. We included patients diagnosed with cHL from 2007 to 2020, initially treated with ABVD, with available baseline PET for review, and with at least two FDG avid lesions. Patients with available RNA from diagnostic biopsy were eligible for gene expression analysis. Dmax was deduced from the three-dimensional coordinates of the baseline metabolic tumor volume (MTV) and its effect on progression free survival (PFS) was evaluated. Gene expression profiles were correlated

Rexhep Durmo and Benedetta Donati equally contributed to this work.

This is an open access article under the terms of the Creative Commons Attribution-NonCommercial License, which permits use, distribution and reproduction in any medium, provided the original work is properly cited and is not used for commercial purposes.

© 2022 The Authors. Hematological Oncology published by John Wiley & Sons Ltd. -

with Dmax and analyzed using CIBERSORTx algorithm to perform deconvolution. The study was conducted on 155 eligible cHL patients. Using its median value of 20 cm, Dmax was the only variable independently associated with PFS (HR = 2.70, 95% CI 1.1–6.63, pValue = 0.03) in multivariate analysis of PFS for all patients and for those with early complete metabolic response (iPET-). Among patients with iPET-low Dmax was associated with a 4-year PFS of 90% (95% CI 82.0–98.9) significantly better compared to high Dmax (4-year PFS 72.4%, 95% CI 61.9–84.6). From the analysis of gene expression profiles differences in Dmax were mostly associated with variations in the expression of microenvironmental components. In conclusion our results support tumor dissemination measured through Dmax as novel prognostic factor for cHL patients treated with ABVD.

#### KEYWORDS

Dmax, gene expression profiling, Hodgkin's lymphoma, PET, tumor dissemination, tumor microenvironment

## 1 | INTRODUCTION

Classical Hodgkin lymphoma (cHL) is a lymphoid neoplasm characterized by varied disease presentation and is accounted as one of the most curable cancers in humans.<sup>1</sup> The current approach to cHL patients requires an accurate assessment of the trade-off between the intensity of the initial treatment and its safety. ABVD (doxorubicin, bleomycin, vinblastine, and dacarbazine) combination with or without radiotherapy is considered a standard regimen for HL due to its excellent tolerability. However, approximately 30% of patients relapse or are refractory to ABVD therapy requiring intensive and toxic salvage therapies.<sup>2</sup> The early identification of patients who are a high risk of treatment failure currently represent an open research question.<sup>3</sup>

Fluorine-18-fluorodeoxyglucose positron emission tomography/computed tomography (<sup>18</sup>F-FDG PET/CT) is a non-invasive tool useful for staging and treatment response purposes in HL.<sup>4</sup> Interim FDG PET/CT (iPET) performed after 2 cycles of chemotherapy is currently used for early assessment of response and to tailor treatment intensity.<sup>5–8</sup> Although highly prognostic, the accuracy of iPET as predictive factor is still suboptimal mainly due to the non-negligible risk of relapse observed among iPET negative (iPET-) patients.<sup>9</sup> Thus, clinical research is currently aimed at identifying additional prognostic factors among those available at time of diagnosis, that may help to increase the accuracy of individual risk prediction. Radiomic features measured at baseline by PET like metabolic tumor volume (MTV), total lesion glycolysis (TLG) and maximum standardized uptake value (SUV-max) have been proposed as promising prognostic biomarker in lymphoma.<sup>10</sup> However, a definitive consensus has not been achieved.<sup>11,12</sup> Among them, the distance between the two lesions that are the furthest apart (Dmax), that reflects lesion dissemination, has gained momentum based on new promising results. Indeed a recent study reported that in Diffuse Large B Cell Lymphoma (DLBCL) the combination of Dmax and MTV identified a group of high-risk patients before treatment.<sup>13,14</sup>

In order to assess the prognostic impact of Dmax in cHL, we conducted a retrospective study in a series of consecutive newly diagnosed patients with confirmed cHL who were treated at our institution with ABVD chemotherapy. We also explored the molecular bases underlying tumor dissemination defined by Dmax through a gene expression analysis on diagnostic biopsies of cHL patients.

## 2 | METHODS

### 2.1 | Patients selection

This study was conducted as a monocentric retrospective analysis. We included patients with confirmed cHL diagnosed in our institution between 2007 and 2020, who were initially treated with ABVD, who had available baseline FDG-PET (bPET) and a minimum follow up of 6 months from diagnosis. Upon centralized review patients with a single lesion at baseline PET were excluded. The main study endpoint was progression free survival (PFS).

This study was conducted in accordance with Declaration of Helsinki and approved by the Internal Review Board. Written consent was obtained from all living patients.

### 2.2 | FDG PET/CT imaging and interpretation

bPET and iPET for all patients were revised by two expert nuclear medicine physicians (RD, AV) who were blinded to patient outcome. PET scanning was performed according to the Society of Nuclear Medicine and Molecular Imaging (SNMMI) and European Association of Nuclear Medicine (EANM) guidelines.<sup>15,16</sup> MTV was calculated for bPET using Beth Israel PET/CT viewer plugin for FIJI (<http://petct-viewer.org>) and defined using the 41% SUVmax threshold. Total

lesion glycolysis was calculated mathematically as the sum of MTV x SUV<sub>mean</sub> of each lesion. Bone marrow involvement was included in the volume measurement only if there was focal uptake as previously described.<sup>17</sup> The centroid was obtained from the three-dimensional coordinates of MTV of each lymphoma lesion. The distances between all pairs of lesions (including both nodal and extra nodal) were calculated by Euclidean formula with LIFEx software.<sup>18</sup> The largest lesion distance was deduced in each patient (Dmax).

iPET was classified according to Deauville Score (DS) as originally reported<sup>19</sup> and interpreted according to Lugano criteria.<sup>4</sup> Body Surface Area (BSA) was calculated according to the Du Bois method.<sup>20</sup>

## 2.3 | Gene expression analysis

We evaluated the gene expression profiles by NanoString using the PanCancer Immune Profiling Panel (NanoString Technologies) as previously described<sup>21,22</sup> starting from  $N = 5$ , 5  $\mu\text{m}$  FFPE slides including whole tissue.

We compared the expression profiles of patients with low- and high-Dmax. pValue (as two-tailed Student's *t* test) and the false discovery rate (FDR) obtained by the Benjamini-Hochberg method were calculated. Bioinformatic analyses were conducted by R Software v4.0.4 packages. Gene expression profiles data are available at the Gene Expression Omnibus (GEO) repository (accession number: GSE184662).

## 2.4 | CIBERSORT analysis

CIBERSORTx algorithm (<https://cibersortx.stanford.edu/>)<sup>23</sup> was used to perform deconvolution of bulk expression data derived from 126 cHL. A 1016-gene customized signature matrix was built as previously described<sup>24</sup> (Supplementary Table S1). Bulk-mode batch correction was applied to mixture samples before imputing cell fractions and 1000 permutations were set for significance analysis. Patients were stratified based on Dmax median value (20 cm). Significantly different infiltrate percentage between the two groups was evaluated for each cell type by Mann-Whitney *U* test.

## 2.5 | Statistical analysis

Associations between clinical variables and radiomic features and Dmax values were evaluated using Fisher's exact test for univariate analysis and by generalized linear model for multivariate analysis.

OS and PFS were estimated with Kaplan-Meier curves and log-rank test was used to assess statistical significance. Cox proportional-hazards model was used for univariate and multivariate survival analysis. For internal validation of Dmax cutoff we first applied Leave One Out cross validation and we calculated the best cutoff of Dmax, TMTV, TLG and SUVmax to predict PFS with

two alternative methods: (1) by using ROC-AUC at 36 months of follow-up and selecting the cut-off by means of Youden index [<sup>25</sup>]; (2) by using maximally selected log-rank test [<sup>26</sup>]. Both the results were confirmed by 1000 bootstrap resamples. Statistical analysis was performed by R Software 4.0.4.

## 3 | RESULTS

### 3.1 | Patients characteristics

A retrospective consecutive cohort of 183 cHLs treated with ABVD regimen was initially identified. bPET scan was available for 180 of the selected patients. Furthermore, 25 patients had a single lesion and were excluded. Thus 155 patients were fully eligible (Figure 1A). Baseline characteristics of eligible patients are reported in Supplementary Table S2.

All patients were evaluated with iPET after 2 cycles of ABVD treatment. iPET was positive for 27 patients (17.4%) and negative for the remaining 128 cases (82.6%). Among the iPET positive patients, treatment was intensified in 10 cases (37.0%), of whom 8 received BEACOPP and 2 IGEV followed by ASCT. A total of 50/155 patients (32.3%) received consolidation radiotherapy (RT) after systemic chemotherapy (Supplementary Table 3). Response to the induction treatment defined by final PET (fPET) was available in 153 patients and was confirmed as CMR in 133 patients (86.9%) and non-CMR in 20 (13.1%).

Radiomic features based on bPET were evaluated and are reported in Supplementary Table S2. Median SUVmax was 14 (IQR: 10–17). Median baseline MTV was 100 cm<sup>3</sup> (IQR: 47–184). Median baseline TLG was 583 (IQR: 267–1265). The agreement between two operators who revised PET images was excellent (Pearson  $r = 0.92$ ,  $p < 0.001$ ).

### 3.2 | Analysis of Dmax and correlation with baseline patient features

Median Dmax was 20 cm (IQR: 11–38). Patients were classified as low-Dmax (Dmax  $\leq 20$  cm) and high-Dmax (Dmax  $> 20$  cm). Dmax value was not influenced by BSA, as demonstrated by correlation plot ( $R = 0.99$ ,  $p < 0.001$ ) (Supplementary Figure 1A–B). In univariate analysis features correlated to high Dmax values were male gender, low serum albumin, low LDH, high ESR and stage. We also observed a direct correlation of Dmax with MTV and TLG. By contrast, no association between Dmax and SUVmax or iPET response was observed (Table 1). Multivariate logistic analysis confirmed the correlation with high Dmax values only for MTV ( $p = 0.003$ ). Different median Dmax values were observed for patients with early or advanced stage defined according to EORTC criteria: 12 cm (IQR: 8–18) and 37 cm (IQR: 22–54), respectively. Distribution of Dmax according to stage is reported in Supplementary Figure 1C.

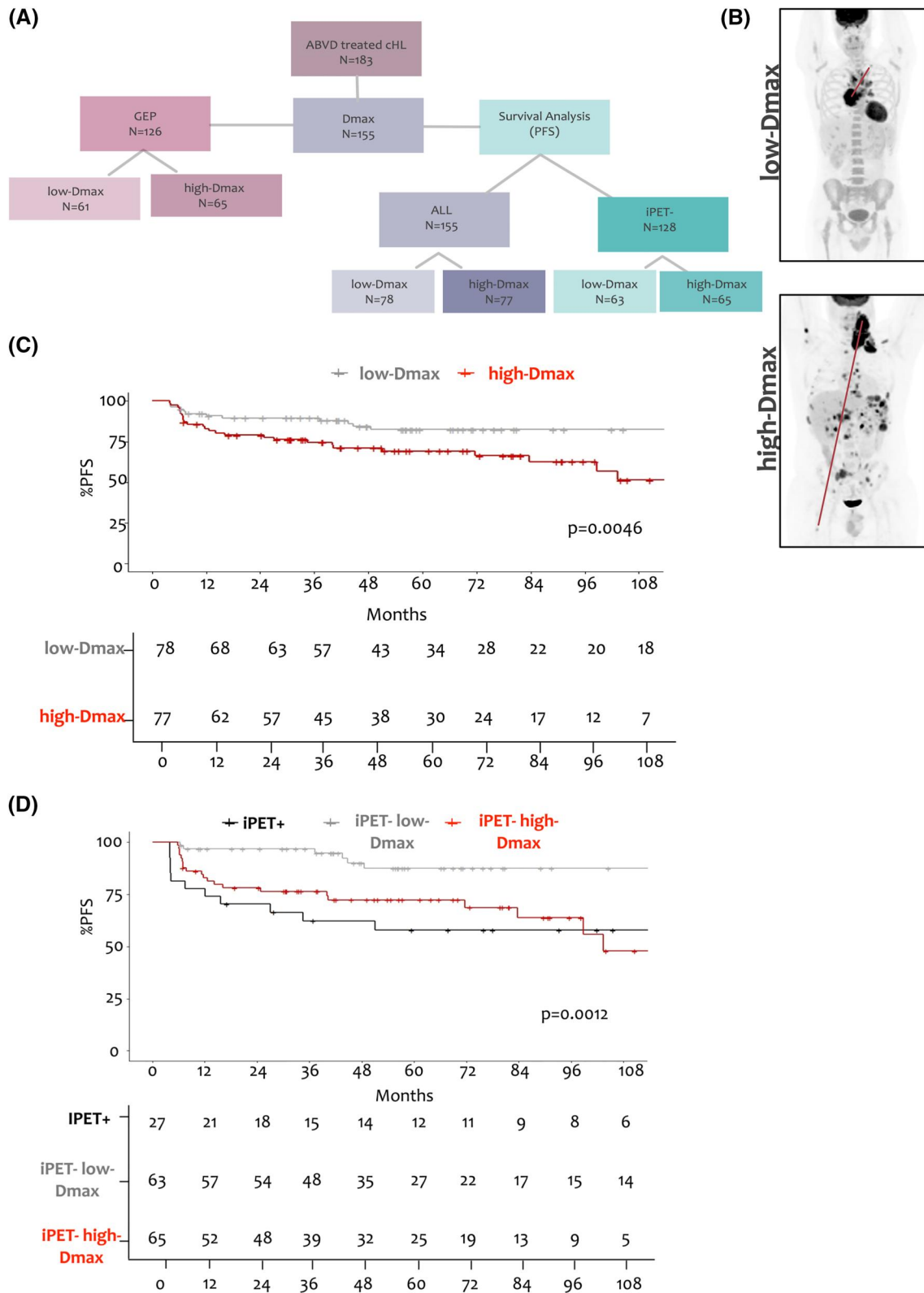


**FIGURE 1** Association of Dmax with progression free survival (PFS) in classical Hodgkin Lymphoma (cHL). (A) Outline of the study (B) PET/CT scan representative of the largest lesions distance defined as low-Dmax (left) and high-Dmax (right) calculated in cHL patients having at least 2 detectable lesions. Red arrows indicate the lesions taken into account (C) Kaplan-Meier curves for PFS among cHL patients with high- and low-Dmax defined on the basis of the median value (20 cm) (D) Kaplan-Meier curves for PFS in the overall cHL cohort among iPET+ and iPET-patients with high- and low-Dmax

TABLE 1 Association of Dmax with clinical-pathological variables in classical Hodgkin Lymphoma (cHL) patients ( $n = 155$ )

	Dmax $\leq 20$ cm (N = 78)	Dmax $> 20$ cm (N = 77)	NA	pValue	Multiv. pValue
Gender			-	0.006	0.109
Female	47 (60.3%)	29 (37.7%)			
Male	31 (39.7%)	48 (62.3%)			
Age			-	0.640	-
$\leq 65$	69 (88.5%)	66 (85.7%)			
$> 65$	9 (11.5%)	11 (14.3%)			
Age			-	0.624	-
$\leq 45$	49 (62.8%)	45 (58.4%)			
$> 45$	29 (37.2%)	32 (41.6%)			
LMR			1	0.333	-
$\leq 2.1$	33 (42.3%)	39 (51.3%)			
$> 2.1$	45 (57.7%)	37 (48.7%)			
Albumin			19	0.017	0.739
$\leq 4$ g/dl	40 (58.0%)	52 (77.6%)			
$> 4$ g/dl	29 (42.0%)	15 (22.4%)			
Hemoglobin			2	0.102	-
$\leq 10.5$ g/dl	7 (9.0%)	14 (18.2%)			
$> 10.5$ g/dl	71 (91.0%)	61 (81.3%)			
Leukocytes			2	0.059	-
$\leq 15 \times 10^3$ cells/mm <sup>3</sup>	74 (94.9%)	64 (85.3%)			
$> 15 \times 10^3$ cells/mm <sup>3</sup>	4 (5.1%)	11 (14.7%)			
LDH/ULN			6	0.013	0.244
$\leq 1$	52 (68.4%)	35 (47.9%)			
$> 1$	24 (31.6%)	38 (52.1%)			
ESR			9	0.004	0.699
$\leq 50$	40 (54.8%)	22 (30.1%)			
$> 50$	33 (45.2%)	51 (69.9%)			
STAGE			-	$< 0.001$	0.991
II	62 (79.5%)	15 (19.5%)			
III	4 (5.1%)	19 (24.7%)			
IV	12 (15.4%)	43 (55.8%)			
Bulky <sup>a</sup>			-	0.383	-
No	63 (80.8%)	67 (87.0%)			
Yes	15 (19.2%)	10 (13.0%)			
Risk group				$< 0.001$	0.449
Local	60 (76.9%)	13 (16.9%)			
Advanced	18 (23.1%)	64 (83.1%)			
HASENCLEVER			-	$< 0.001$	0.294
0-2	59 (75.6%)	32 (41.6%)			
$> 2$	19 (24.4%)	45 (58.4%)			

(Continues)

TABLE 1 (Continued)

	Dmax ≤20 cm (N = 78)	Dmax >20 cm (N = 77)	NA	pValue	Multiv. pValue
MTV			-	<0.001	0.003
≤100 cm <sup>3</sup>	57 (73.1%)	20 (26.0%)			
>100 cm <sup>3</sup>	21 (26.9%)	57 (74.0%)			
TLG			-	<0.001	0.140
≤583	52 (66.7%)	24 (31.2%)			
>583	26 (33.3%)	53 (68.8%)			
SUVmax			-	0.200	-
≤14	45 (57.7%)	36 (46.8%)			
>14	33 (42.3%)	41 (53.2%)			
iPET			-	0.673	-
Pos	15 (19.2%)	12 (15.6%)			
Neg	63 (80.8%)	65 (84.4%)			

Note: LMR, lymphocytes/monocytes ratio; LDH, Lactate dehydrogenase; ULN, upper limit normal; ERS, erythrocytes sedimentation rate; MTV, total tumor metabolic volume; SUV, standardized uptake value; TLG, total lesion glycolysis; Dmax, largest distance between the two most distant lesions. Univariate pValue was calculated as two-tailed Fisher exact test. Multivariate pValue, including variables significantly associated with Dmax at univariate analysis, was calculated by generalized linear model (glm). The pValues shown in boldface correspond to  $p < 0.05$ .

<sup>a</sup>Bulky was any lesion greater than 10 cm in one of transverse diameters measured on a CE-CT scan.

### 3.3 | Dmax correlation with survival probability

Median follow-up of the cohort was 63 months (range, 6.5–139 months). 39 patients experienced an event for PFS including 29 disease progressions and 10 deaths. The 4-year PFS rate was 77.7% (95%CI 71.1–84.9). Considering Overall Survival (OS), 13 patients died of whom 4 due to lymphoma progression and 9 due to other causes resulting in a 4-year OS rate of 92.9% (95% CI 88.5–97.5).

To establish the prognostic value of radiomic features in CHL, we evaluated the risk of disease progression (as PFS) associated to the median value of each parameter by Cox regression hazard model. In univariate analysis, no significant correlation was observed for MTV, TLG and SUVmax for the whole series. A significant correlation between MTV and PFS was observed when analysis was limited to patients younger than 60 years and adjusted for the main clinical risk factors (HR 2.66, 95%CI 1.11–6.38). By contrast, high Dmax was significantly associated with increased risk of disease progression (HR = 2.59, 95%CI 1.31–5.12) (Table 2). Indeed, patients with low Dmax had a 4 years PFS of 84.3% (95%CI 76.0–93.4), significantly better than patients with high Dmax (4 years PFS: 71.1%, 95%CI to 82.5%) (Figure 1C). Dmax confirmed its prognostic role also when considered as a continues variable (HR 1.54, 95%CI 1.03–2.32) and also when corrected for BSA (Supplementary Figure 1B).

Among clinical variables, advanced stage (AA III-IV) (HR = 1.93, 95% CI 1–3.73) and iPET positivity (HR = 1.95, 95% CI 0.97–3.93) showed a significant association with reduced PFS (Table 2). Multivariate analysis for PFS showed that Dmax was the only variable remaining associated with disease progression, confirming the independent prognostic role of this metabolic parameter (HR = 2.70, 95% CI 1.1–6.63). These results were confirmed when the multivariate

model was corrected for RT consolidation and for treatment intensification in iPET + patients (HR = 2.50, 95%CI 1.20–5.21) (Table 2).

### 3.4 | Combined analysis of Dmax and iPET

We evaluated the prognostic role of Dmax for patients who achieved a negative iPET and continued their treatment with ABVD chemotherapy. In this group high Dmax significantly increased the risk of progression (HR = 4.53, 95%CI 1.81–11.3) and this association was confirmed in a multivariate analysis including Stage (III-IV) as covariate (HR = 4.98, 95%CI 1.64–15.16). These results were also confirmed when the multivariate model was corrected for consolidation radiotherapy (HR = 3.96, 95%CI 1.52–10.33) (Table 3).

Combining Dmax and iPET we observed that Dmax was able to identify patients at different risk of progression only among iPET-patients, while no additional prognostic role was seen for the small group of iPET + cases. Thus, combining iPET and Dmax we were able to identify three risk groups (Figure 1D). Sixty-three (41%) patients had iPET- and low Dmax and a 4 years PFS of 90% (95%CI 82.0–98.9) significantly better compared to the 65 (42%) patients with iPET- and high Dmax (4 years PFS 72.4% (95%CI 61.9–84.6)). The 27 (17%) patients with a positive iPET had a 4 years PFS of 62.3% (95%CI 46.3–83.9).

### 3.5 | Internal validation of Dmax prognostic cut-off

To avoid data overfitting, due to the limited sample size and a low number of events, we used the median value of our cohort to analyze

**TABLE 2** Cox Model for progression free survival (PFS) analysis in the classical Hodgkin Lymphoma (cHL) cohort ( $n = 155$ )

	Univariate analysis		Multivariate analysis		Adj. For treatment	
	HR (95%CI)	pValue	HR (95%CI)	pValue	HR (95%CI)	pValue
Age ( $\geq 65$ )	1.75 (0.80–3.80)	0.159	-	-	-	-
Age ( $\geq 45$ )	1.16 (0.62–2.18)	0.647	-	-	-	-
Stage (III-IV)	1.93 (1.00–3.73)	<b>0.049</b>	0.93 (0.39–2.23)	0.872	-	-
Bulky (yes)	0.68 (0.27–1.75)	0.429	-	-	-	-
LMR ( $\geq 2.1$ )	0.90 (0.48–1.71)	0.756	-	-	-	-
Dmax ( $\geq 20$ cm)	2.59 (1.31–5.12)	<b>0.006</b>	2.70 (1.10–6.63)	<b>0.030</b>	2.50 (1.20–5.21)	<b>0.014</b>
MTV ( $\geq 100$ cm <sup>3</sup> )	1.50 (0.79–2.83)	0.217	-	-	-	-
TLG ( $\geq 583$ )	1.21 (0.64–2.29)	0.550	-	-	-	-
SUVmax ( $\geq 14$ )	1.10 (0.59–2.07)	0.758	-	-	-	-
iPET (pos)	1.95 (0.97–3.93)	0.063	1.97 (0.96–4.07)	0.066	1.37 (0.59–3.19)	0.467

Note: LMR, lymphocytes/monocytes ratio; MTV, tumor metabolic volume; SUV, standardized uptake value; TLG, total lesion glycolysis; Dmax, largest distance between the two most distant lesions. Multivariate Cox model includes variables resulted significant at the univariate analysis. pValue adjusted for treatment includes therapy escalation and radiotherapy. The pValues shown in boldface correspond to  $p < 0.05$ .

**TABLE 3** Cox Model for progression free survival (PFS) analysis in the iPET negative classical Hodgkin Lymphoma (cHL) cohort ( $n = 128$ )

	Univariate analysis		Multivariate analysis		Adj. For treatment	
	HR (95%CI)	pValue	HR (95%CI)	pValue	HR (95%CI)	pValue
Age ( $\geq 65$ )	1.93 (0.82–4.55)	0.132	-	-	-	-
Age ( $\geq 45$ )	1.55 (0.74–3.26)	0.245	-	-	-	-
Stage (III-IV)	2.27 (1.04–4.97)	<b>0.039</b>	0.87 (0.34–2.23)	0.766	-	-
Bulky (yes)	0.63 (0.19–2.09)	0.450	-	-	-	-
LMR ( $\geq 2.1$ )	0.88 (0.41–1.87)	0.732	-	-	-	-
Dmax ( $\geq 20$ cm)	4.53 (1.81–11.3)	<b>0.001</b>	4.98 (1.64–15.16)	<b>0.005</b>	3.96 (1.52–10.33)	<b>0.005</b>
MTV ( $\geq 100$ cm <sup>3</sup> )	1.50 (0.71–3.18)	0.289	-	-	-	-
TLG ( $\geq 583$ )	1.19 (0.56–2.51)	0.647	-	-	-	-
SUVmax ( $\geq 14$ )	0.74 (0.34–1.61)	0.447	-	-	-	-

Note: LMR, lymphocytes/monocytes ratio; MTV, tumor metabolic volume; SUV, standardized uptake value; TLG, total lesion glycolysis; Dmax, largest distance between the two most distant lesions. Multivariate Cox model includes variables resulted significant at the univariate analysis. pValue adjusted for treatment includes radiotherapy. The pValues shown in boldface correspond to  $p < 0.05$ .

the prognostic role of Dmax. However, we applied different approaches to provide an internal validation of our observations and to strength the reliability of this Dmax cut-off.

First, Leave One Out (LOO) internal validation showed a repeatable performance of this cut-off, indeed original Dmax  $> 20$  cm and LOO Dmax  $> 20$  cm had HR of 2.59 (95% CI 1.31–5.11) and 2.38 (95% CI 1.18–4.78) with a Gohen/Heller Concordance of 0.61 (SE 0.04) and 0.59 (SE 0.04), respectively. Then, with the Dmax as continuous value, we evaluated the ROC-AUC at 36 months of follow-up (3 years) in the overall cohort (AUC = 0.57) and we selected the cut-point of 19.4 by means of Youden index (Figure 2A). After 1000 bootstrap resamples the 2.5–97.5 percentiles were 16.6–20.7 with a bias of 0.40. Furthermore, we took advantages of a second approach to define Dmax cutoff on the overall cohort based

on maximally selected log-rank test. Even in this case we obtained an estimated cut point of 19.4 cm ( $p = 0.029$ ), that was confirmed also after 1000 bootstrapped resamples (Bias  $-0.0036$ , 2.5–97.5 percentiles were 10.4–21.8) (Figure 2B and C). All together these analyses indicate that the Dmax  $> 20$  cm is an accurate threshold within our cohort. A similar approach was used to validate cut-offs for TMTV, TLG and SUVmax (Supplementary Figure 2).

### 3.6 | Gene expression profiling and CIBERSORT analysis

We employed digital profiling for investigating the biological bases of Dmax. 126 of the 155 cHLs analyzed samples had biological material

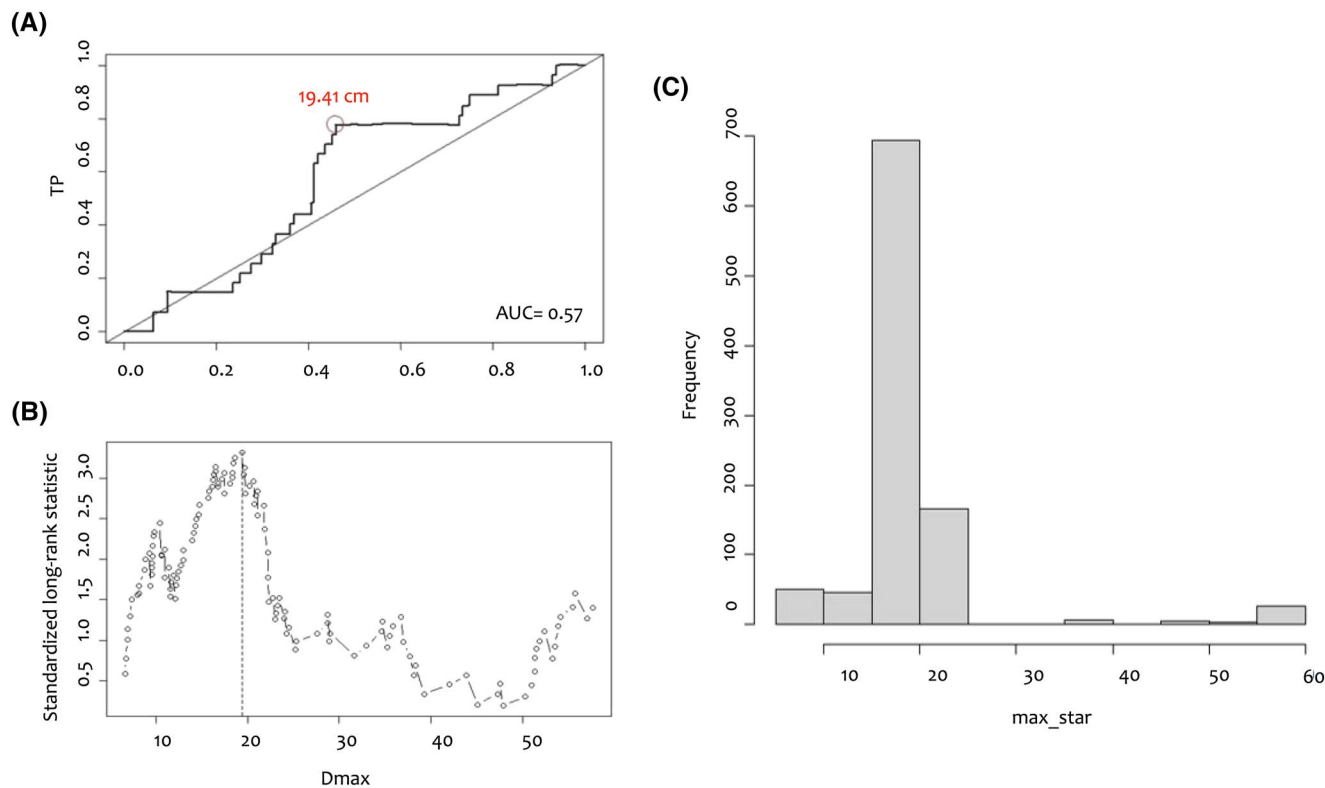


**FIGURE 2** Validation of Dmax cut-off (A) Definition of Dmax Cut-off by means of ROC curve. methods and Youden index considering 36 months of follow up (B) Definition of Dmax Cut-off by means of maximally selected log-rank test. (C) Histogram of max.star representing 1000 bootstrapped resamples

suitable for the analysis. Of these, 61 (48.4%) were low-Dmax and 65 (51.6%) were high-Dmax (Figure 1A).

556 of the evaluated genes were expressed in at least one of the two groups. Differential analysis of the gene expression profiles between the high- and low-Dmax groups resulted in 154 differentially expressed genes, of which 46 (29.8%) upregulated and 108 (70.2%) downregulated in high-Dmax (Figure 3A). After *p*-value adjustment, 61 genes remained differentially distributed between the two groups. Principal Component Analysis (PCA) showed that gene expression profiles partially segregated high and low-Dmax samples (Figure 3B). 21 genes were up-regulated and 40 down-regulated in high-Dmax versus low-Dmax samples (Figure 3C).

Gene Ontology analysis showed that down-regulated genes in high Dmax samples were particularly enriched in processes linked to T- and B- cells homeostasis, activation and mediated cell response (Figure 4A). Of note, among the others, expression of B-cell specific markers like CD20 (MS4A1) and CD79A-B and T-cell specific factors like FOXP3 resulted significantly downregulated in high-Dmax patients. By contrast, among the up-regulated genes we observed the macrophage-specific marker CD68 ( $\log_2(\text{FC}) = 0.41$ , *adj. pValue* = 0.05) and several macrophage-associated factors including CXCL9, CCL24, CD163, CD14 and MRC1 (Figure 3C).

A deconvolution approach was used to infer the cell populations associated to Dmax on the basis of gene expression profiling.<sup>23</sup> HL cells, B cells, CD8+ and CD4+ T cells were the predominant cell populations in our samples. Also, vascular

components including endothelial cells, pericytes and myofibroblasts were well represented. Differential analysis of the distribution of these cell populations showed that naïve B and T cells were strongly enriched in the low-Dmax subgroup. By contrast CD8+ T cells expressing high level of PDL1, dendritic cells, monocytes and eosinophil were enriched in the high-Dmax samples. Even if poorly represented in the tumor microenvironment, Cancer Associated Fibroblasts (CAFs) resulted also to be preferentially associated with low Dmax (Figure 4B and Supplementary Table 4). No differences in the distribution of HL cells was observed between high and low-Dmax cases. We also explored how the 7 Dmax-associated cytotypes correlate with other PET parameters (Supplementary Figure 3A–D). The median value of TMTV and TLG was significantly associated with 5 and 4 cell subsets, respectively, whereas SUVmax only correlated with monocytes. Moreover, the whole panel of cytotypes showed a prognostic trend in term of PFS, which was statistically significant for naïve B cells and CD8+/highPDL1 T cells, in a way consistent with their association to Dmax (Supplementary Figure 3E–F).

## 4 | DISCUSSION

In this study we evaluated the prognostic role of tumor spread defined by Dmax, a simple measurement of the largest distance between lymphoma sites, in a retrospective cohort of consecutive



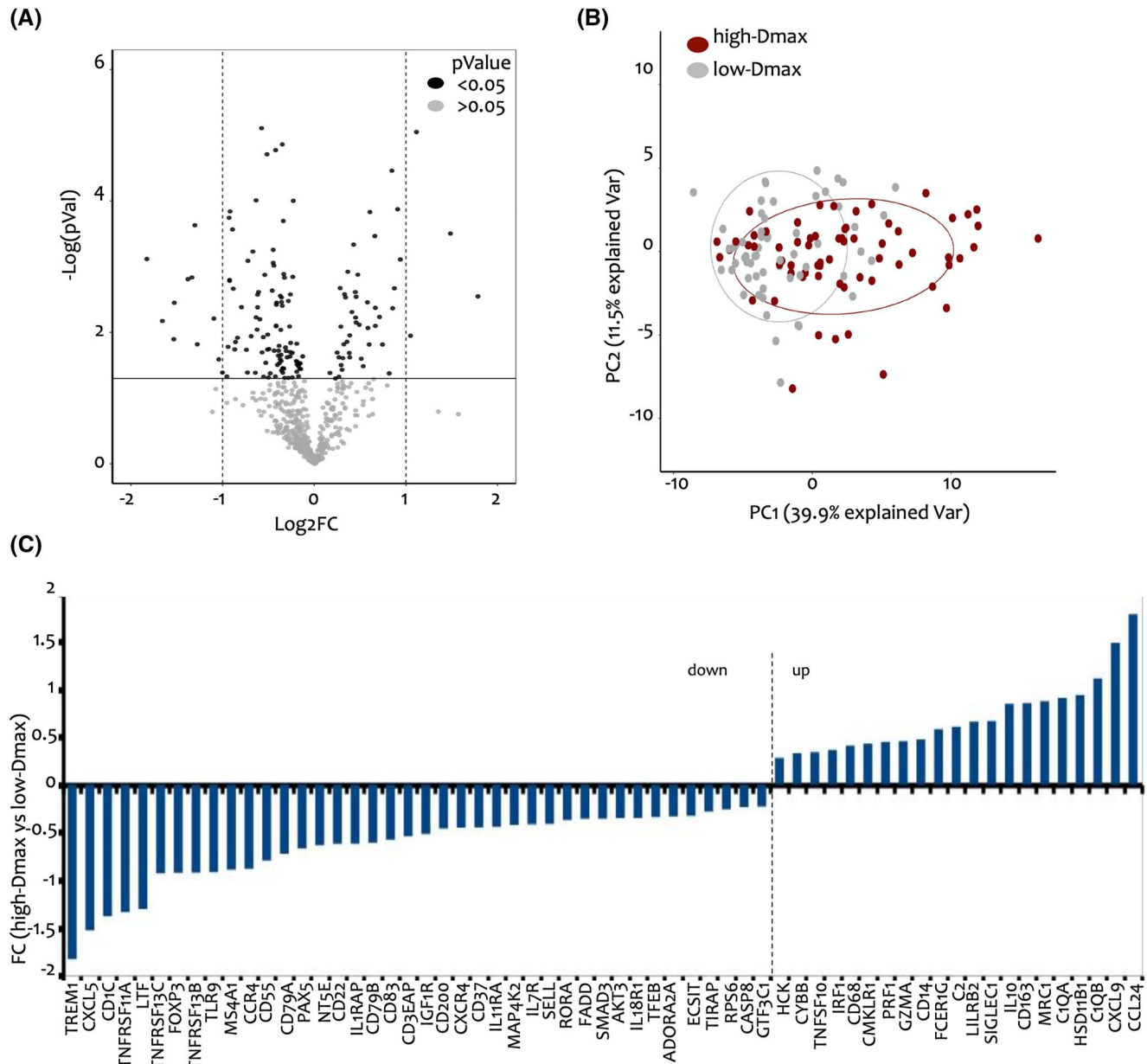


**FIGURE 3** Gene expression analysis associated to tumor dissemination. (A) Volcano plot displaying differential expressed genes between classical Hodgkin Lymphoma (cHL) patients with high- and low-Dmax. Black dots represent genes significantly deregulated ( $p\text{Value} \leq 0.05$ ) and dotted lines indicate absolute  $\text{FC} \geq 2$ . (B) Principal Component Analysis (PCA) shows the variance between high- (red dots) and low- (gray dots) Dmax samples explained by the 61 genes differentially expressed with  $\text{FDR} \leq 0.05$ . (C) Histogram representing Fold Change (FC) of the 61 genes differentially expressed ( $\text{FDR} \leq 0.05$ ) in high-versus low- Dmax samples

newly diagnosed patients with cHL treated with ABVD. We were able to demonstrate the independent correlation of Dmax with the risk of progression for all patients included in the study and for the subgroup of patients who achieved a CMR early during the treatment course with a five-fold increase in the risk of disease progression associated with high Dmax compared to low Dmax.

Our study should be considered as a proof of concept about the prognostic role of Dmax in cHL that may have some implications related to the initial evaluation of patients and for the future development of risk adapted therapies in cHL. In spite of the relevant

progresses gained in the recent years in the understanding and evaluation of disease features, still staging and consequential management of cHL are relying on historical qualitative criteria, that poorly account for the complex biology of this tumor.

Compared to standard Ann Arbor staging that failed to predict outcome in our study, as well as in other studies,<sup>13</sup> Dmax appeared more effective for risk stratification. Indeed, according to our analysis, Dmax contributes to a more precise evaluation of tumor spreading compared to Ann Arbor index, in particular for patients at intermediate risk.

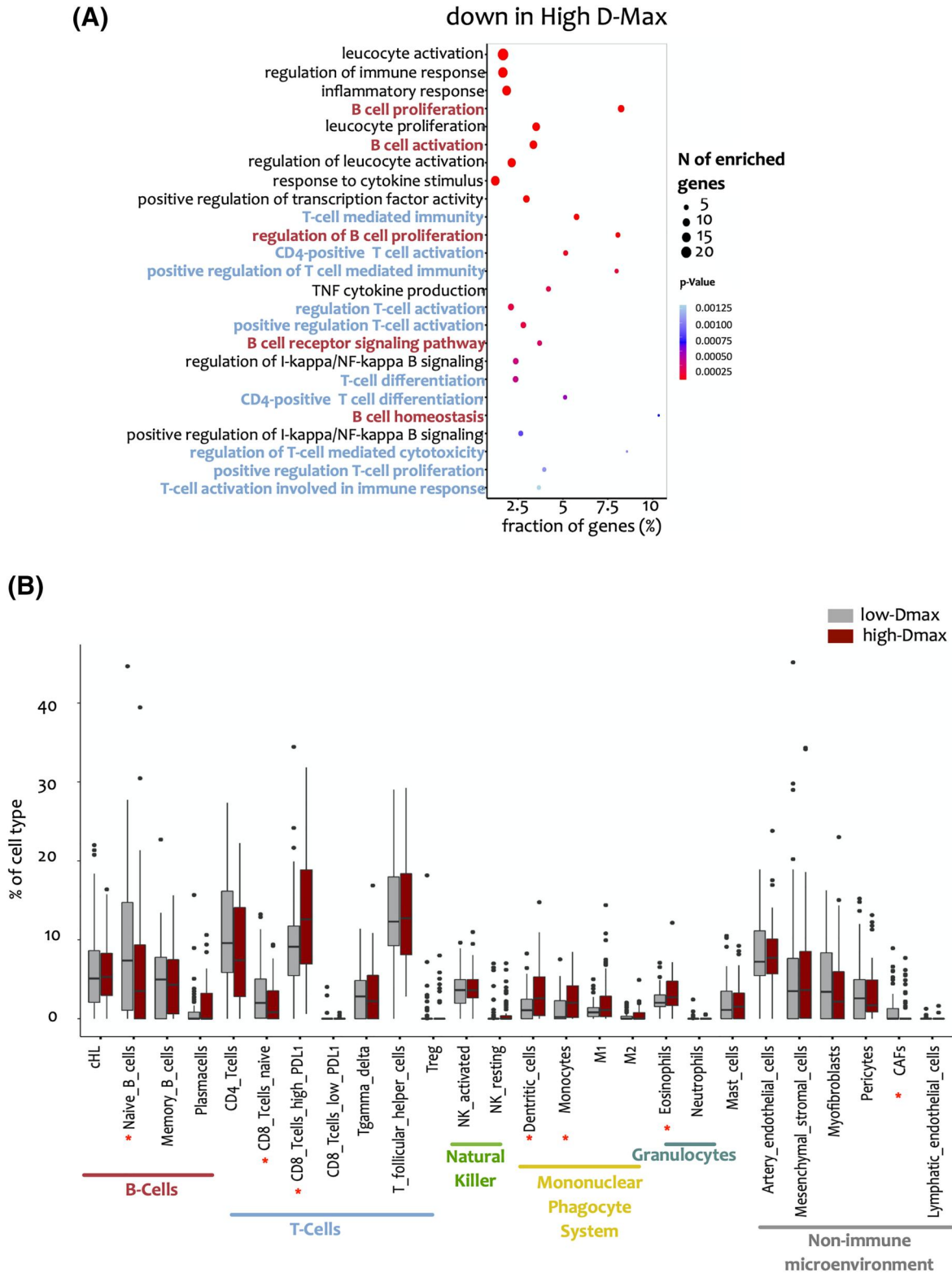


**FIGURE 4** Cell populations associated to tumor dissemination (A) GO analysis of the 40 genes down-regulated in high-versus low-Dmax samples. B-cells related and T-cells related pathways are highlighted in red and blue respectively (B) Box plot representing the distribution of cell populations analyzed by CIBERSORTx among high- and low- Dmax samples

Diagnostic imaging features collected at diagnosis by PET are regarded as potential source of relevant prognosis indicators. We showed that, differently from other radiomic parameters, including

MTV, TLG and SUVmax, whose prognostic value was not confirmed by our analysis, Dmax had an independent association with the risk of progression and was confirmed in the subgroup of early responding

patients. Noticeably, Dmax is a very simple feature to calculate, that is measured as the distance between centroids of two lesions, that is not impacted by the scanner or the operator, differently from the other PET-derived features.

Regarding the contribution of Dmax to response adapted therapy in cHL patients, a major finding of our analysis was the evidence that Dmax is an independent prognostic factor for PFS among the iPET-patients. Indeed, an unsolved need is currently identified in the non-negligible proportion of early responding patients who still experience relapse after completion of front-line therapy, regardless of initial stage. The risk of disease progression reflects some innate features of the tumor that are not captured by standard prognostic factors but can be partly revealed by the analysis of Dmax.

Being an index of tumor spreading, Dmax may be considered as a surrogate of tumor aggressiveness. To map this connection, we employed digital gene expression profiling to investigate the biologic features of Dmax at diagnosis.

We chose to not confining the analysis to Reed-Sternberg (RS) cells but to consider whole tumor tissue since, in cHL tumor microenvironment accounts for a significant part of the biology of the disease and its behavior.<sup>27</sup> We used the same approach in our previous work demonstrating that microenvironmental dynamics concur to define innate chemorefractoriness to ABVD.<sup>21</sup> Therefore, our explorative study represents an attempt to link peculiar aspects of cHL microenvironment to Dmax as a measure of the proneness of tumor to spread during progression. While we recognize the use of a limited panel of genes as a limitation of our analysis, the obtained profiles were able to partly segregate high and low Dmax lesions. Genes associate to low-Dmax, were representative of pathways related to B-cells and T-cells presence and activation (Figure 3B–C). In particular, B-cells specific markers like CD20 (encoded by MS4A1 gene), CD79 A and B were significantly overexpressed in low-Dmax lesions. Also, lineage committing transcription factor like PAX5<sup>28</sup> and FOXP3,<sup>29,30</sup> were significantly overexpressed in low-Dmax cHLs. By contrast, expression of macrophages/monocytes markers including CD68, CD163 resulted associated to high-Dmax lesions, coherent with a general role of these cells in tumor progression.<sup>31</sup> Of note the expression of FOXP3, CD68 and CD20 in the tumor microenvironment has been already reported to have a prognostic value in cHLs.<sup>32</sup> In particular, high expression of FOXP3 and CD20 at diagnosis were reported to be associated to superior OS, while increased levels of CD68 were predictive of increased first-line treatment failure and reduce OS. Our results are coherent with these observations and add a new layer of information suggesting that this peculiar asset of the tumor microenvironment may contribute to cHL progression by creating favorable conditions to tumor dissemination.

Deconvolution analysis by CIBERSORTx confirmed this evidence. Indeed, higher Dmax characterizes those cHL with an under-represented immune microenvironment, particularly in naïve B cells and CD8+ T cells compartments. Interestingly, a subset of CD8+ T effector expressing higher PD-L1 level directly correlated with Dmax, featuring more aggressive disease. As a critical immune checkpoint,

PD-L1 promotes immune-escape<sup>33</sup> and, in keeping with higher infiltration of CD68-positive cells, is negatively associated with cHL patients' survival.<sup>34</sup> This is also in line with the concept that weaker immune response correlates with proneness of distant spreading in many cancer types including B-cell lymphoma.<sup>35,36</sup>

Our results were generated from and should be referred to an unselected population of cHL patients homogeneously treated with ABVD that is the first-choice therapy for the majority of patients around world. The only difference in the treatment protocol was represented by the number of ABVD cycles, by the adoption of consolidation radiotherapy according to available guidelines and by the intensification of treatment for some iPET + patients that was defined on a patient basis and upon multidisciplinary discussion. This choice allowed to include in the study most of the patients seen in our institution and to significantly reduce interferences caused by treatment dependent biases. Indeed, our observation is referred to the majority of patients with the only exclusion of stage I disease who are not eligible for Dmax calculation. However, considering that other options are currently prescribed mostly for patients with advanced disease, larger studies, and a full validation of Dmax in patients treated with regimens other than ABVD are required before our results can be generalized to all cHL patients.

Kanoun et al. recently provided confirmatory data about the prognostic role of Dmax among patients initially treated with BEA-COPP within the AHL2011 randomized trial.<sup>37</sup> Also, regarding the cut-off value of Dmax that was defined at 20 cm in our study further validation is needed. Indeed, our data should be considered as a proof of concept about the prognostic role of Dmax in cHL patients and to identify subgroups of patients that could have the greater utility from the use of Dmax, that is, iPET negative patients. We acknowledge all the limitations of our study population in term of size and representativeness. However, we also believe that our conclusions are well supported by data. Larger trials with well-defined validation cohort will be needed to define the best cut off for Dmax that will likely be different for different risk subgroups.

Among study results the lack of prognostic value for MTV or TLG was in contrast with available data.<sup>38</sup> Indeed, neither MTV or TLG were confirmed as prognostic factors for the whole patients series in the univariate analysis of PFS and were not analyzed in the multivariate model. The small sample size and the few observed events reported in our study might be a reasonable explanation to this discordancy. Indeed an association between MTV with patients' outcome was found when the analysis was limited to patients younger than 60 years suggesting the presence of biases associated with older patients.

In conclusion, our study suggests Dmax as a relevant feature allowing to better predict patients' outcome among subjects otherwise defined at low risk based on their early response to ABVD chemotherapy. Pending further validation Dmax may be suggested as a new simple assessment that, added to the initial workup of patients, might contribute to a better definition of patient risk profile and to a more precise personalization of therapy in cHL.

## ACKNOWLEDGMENTS

We are grateful to Dr. Luigi Marcheselli for his valuable support to the statistical analysis. We also wish to thank Dr. Savonarola for inspiring our writing. This work was supported by Fondazione Italiana per la Ricerca sul Cancro (AIRC-IG2021- 25802) of Prof Stefano Luminari, and by Fondazione GRADE ONLUS Reggio Emilia to Dr. Alessia Ruffini.

Open Access Funding provided by Universita degli Studi di Modena e Reggio Emilia within the CRUI-CARE Agreement.

## CONFLICT OF INTEREST

No conflict of interest exists related to the content of this manuscript. I.B. received research funding from Siemens Healthineers, General Electric Healthcare and Dosisoft outside the submitted work.

## AUTHOR CONTRIBUTIONS

Stefano Luminari, Alessia Ciarrocchi, Annibale Versari designed research. Rexhep Durmo, Benedetta Donati, Alessia Ruffini, Maria Carmela Vegliante, Louis Rebau performed research. Louis Rebau, Anne Segolene Cottreau, Christophe Nioche, Irene Buvat, Michel Meignan, Sabino Ciavarella, Maria Carmela Vegliante contributed analytical tools. Benedetta Donati, Alessia Ciarrocchi, Rexhep Durmo, Stefano Luminari, Annibale Versari, Francesco Merli, Maria Elena Nizzoli, Sabino Ciavarella, Maria Carmela Vegliante analyzed data. Sabino Ciavarella, Annibale Versari, Michel Meignan supervised the work. Benedetta Donati, Alessia Ciarrocchi, Rexhep Durmo, Stefano Luminari wrote the paper. Annibale Versari, Francesco Merli, Michel Meignan, Sabino Ciavarella, Maria Carmela Vegliante, Irene Buvat, revised and edited the paper. All Authors approved the final version of the manuscript.

## DATA AVAILABILITY STATEMENT

The data that support the findings of this study are openly available in Gene Expression Omnibus (GEO) repository at GEO Accession viewer ([nih.gov](https://www.ncbi.nlm.nih.gov/geo/)) reference number GSE184662.

## ORCID

Maria Carmela Vegliante  <https://orcid.org/0000-0002-3165-1768>

Alessia Ciarrocchi  <https://orcid.org/0000-0002-5541-2075>

## TRANSPARENT PEER REVIEW

The peer review history for this article is available at <https://publons.com/publon/10.1002/hon.3025>.

## REFERENCES

1. Thomas RK, Re D, Zander T, Wolf J, Diehl V. Epidemiology and etiology of Hodgkin's lymphoma. *Ann Oncol*. 2002;13(Suppl 4):147-152. <https://doi.org/10.1093/annonc/mdf652>
2. Viviani S, Zinzani PL, Rambaldi A, et al. ABVD versus BEACOPP for Hodgkin's lymphoma when high-dose salvage is planned. *N Engl J Med*. 2011;365(3):203-212. <https://doi.org/10.1056/nejmoa1100340>
3. Merli F, Luminari S, Gobbi PG, et al. Long-term results of the HD2000 trial comparing ABVD versus BEACOPP versus COPP-EBV-CAD in untreated patients with advanced hodgkin lymphoma: a study by Fondazione Italiana Linfomi. *J Clin Oncol*. 2016;34(11):1175-1181. <https://doi.org/10.1200/jco.2015.62.4817>
4. Cheson BD, Fisher RI, Barrington SF, et al. Recommendations for initial evaluation, staging, and response assessment of hodgkin and non-hodgkin lymphoma: the lugano classification. *J Clin Oncol*. 2014;32(27):3059-3067. <https://doi.org/10.1200/jco.2013.54.8800>
5. Borchmann P, Haverkamp H, Lohri A, et al. Progression-free survival of early interim PET-positive patients with advanced stage Hodgkin's lymphoma treated with BEACOPPescalated alone or in combination with rituximab (HD18): an open-label, international, randomised phase 3 study by the German Hodgk. *Lancet Oncol*. 2017;18(4):454-463. [https://doi.org/10.1016/s1470-2045\(17\)30103-1](https://doi.org/10.1016/s1470-2045(17)30103-1)
6. Kobe C, Goergen H, Baues C, et al. Outcome-based interpretation of early interim PET in advanced-stage Hodgkin lymphoma. *Blood*. 2018;132(21):2273-2279. <https://doi.org/10.1182/blood-2018-05-852129>
7. Straus DJ, Jung SH, Pitcher B, et al. CALGB 50604: risk-adapted treatment of nonbulky early-stage Hodgkin lymphoma based on interim PET. *Blood*. 2018;132(10):1013-1021. <https://doi.org/10.1182/blood-2018-01-827246>
8. Radford J, Illidge T, Counsell N, et al. Results of a trial of PET-directed therapy for early-stage Hodgkin's lymphoma. *N Engl J Med*. 2015;372(17):1598-1607. <https://doi.org/10.1056/nejmoa1408648>
9. Stephens DM, Li H, Schöder H, et al. Five-year follow-up of SWOG S0816: limitations and values of a PET-adapted approach with stage III/IV Hodgkin lymphoma. *Blood*. 2019;134(15):1238-1246. <https://doi.org/10.1182/blood.2019000719>
10. Mettler J, Müller H, Voltin CA, et al. Metabolic tumor volume for response prediction in advanced-stage hodgkin lymphoma. *J Nucl Med*. 2019;60(2):207-211. <https://doi.org/10.2967/jnumed.118.210047>
11. Schöder H, Moskowitz C. Metabolic tumor volume in lymphoma: hype or hope? *J Clin Oncol*. 2016;34(30):3591-3594. <https://doi.org/10.1200/jco.2016.69.3747>
12. Guo B, Tan X, Ke Q, Cen H. Prognostic value of baseline metabolic tumor volume and total lesion glycolysis in patients with lymphoma: a meta-analysis. *PLoS One*. 2019;14(1):e0210224. <https://doi.org/10.1371/journal.pone.0210224>
13. Cottreau A-S, Nioche C, Dirand A-S, et al. 18 F-FDG PET dissemination features in diffuse large B-cell lymphoma are predictive of outcome. *J Nucl Med*. 2020;61(1):40-45. <https://doi.org/10.2967/jnumed.119.229450>
14. Cottreau AS, Meignan M, Nioche C, et al. Risk stratification in diffuse large B-cell lymphoma using lesion dissemination and metabolic tumor burden calculated from baseline PET/CT. *Ann Oncol*. 2021;32(3):404-411. <https://doi.org/10.1016/j.annonc.2020.11.019>
15. Delbeke D, Coleman RE, Guiberteau MJ, et al. Procedure guideline for tumor imaging with 18F-FDG PET/CT 1.0. *J Nucl Med*. 2006;47(5):885-895.
16. Boellaard R, Delgado-Bolton R, Oyen WJG, et al. FDG PET/CT: EANM procedure guidelines for tumour imaging: version 2.0. *Eur J Nucl Med Mol Imag*. 2015;42(2):328-354. <https://doi.org/10.1007/s00259-014-2961-x>
17. Adams HJA, Kwee T, de Keizer B, et al. Systematic review and meta-analysis on the diagnostic performance of FDG-PET/CT in detecting bone marrow involvement in newly diagnosed Hodgkin lymphoma: is bone marrow biopsy still necessary? *Ann Oncol*. 2014;25(5):921-927. <https://doi.org/10.1093/annonc/mdt533>
18. Nioche C, Orhac F, Boughdad S, et al. LIFEX: a freeware for radiomic feature calculation in multimodality imaging to accelerate advances in the characterization of tumor heterogeneity. *Cancer Res*. 2018;78(16):4786-4789. <https://doi.org/10.1158/0008-5472.can-18-0125>
19. Meignan M, Gallamini A, Meignan M, Gallamini A, Haioun C. Report on the first international workshop on interim-PET scan in

- lymphoma. *Leuk Lymphoma*. 2009;50(8):1257-1260. <https://doi.org/10.1080/10428190903040048>
20. Shuter B, Aslani A. Body surface area: Du Bois and Du Bois revisited. *Eur J Appl Physiol*. 2000;82(3):250-254. <https://doi.org/10.1007/s004210050679>
  21. Luminari S, Donati B, Casali M, et al. A gene expression-based model to predict metabolic response after two courses of ABVD in hodgkin lymphoma patients. *Clin Cancer Res*. 2020;26(2):373-383. <https://doi.org/10.1158/1078-0432.ccr-19-2356>
  22. Donati B, Ferrari A, Ruffini A, et al. Gene expression profile unveils diverse biological effect of serum vitamin D in Hodgkin's and diffuse large B-cell lymphoma. *Hematol Oncol*. 2021;39(2):205-214. <https://doi.org/10.1002/hon.2827>
  23. Newman AM, Liu CL, Green MR, et al. Robust enumeration of cell subsets from tissue expression profiles. *Nat Methods*. 2015;12(5):453-457. <https://doi.org/10.1038/nmeth.3337>
  24. Ciavarella S, Vegliante MC, Fabbri M, et al. Dissection of DLBCL microenvironment provides a gene expression-based predictor of survival applicable to formalin-fixed paraffin-embedded tissue. *Ann Oncol*. 2018;29(12):2363-2370. <https://doi.org/10.1093/annonc/mdy450>
  25. Heagerty PJ, Lumley T, Pepe MS. Time-dependent ROC curves for censored survival data and a diagnostic marker. *Biometrics*. 2000;56(2):337-344. <https://doi.org/10.1111/j.0006-341x.2000.00337.x>
  26. Lausen B, Schumacher M. Maximally selected rank statistics. *Biometrics*. 1992;48(1):73. <https://doi.org/10.2307/2532740>
  27. Liu Y, Sattarzadeh A, Diepstra A, Visser L, Van Den Berg A. The microenvironment in classical Hodgkin lymphoma: an actively shaped and essential tumor component. *Semin Cancer Biol*. 2014;24:15-22. <https://doi.org/10.1016/j.semcancer.2013.07.002>
  28. Revilla-I-Domingo R, Bilic I, Vilagos B, et al. The B-cell identity factor Pax5 regulates distinct transcriptional programmes in early and late B lymphopoiesis. *EMBO J*. 2012;31(14):3130-3146. <https://doi.org/10.1038/emboj.2012.155>
  29. Marson A, Kretschmer K, Frampton GM, et al. Foxp3 occupancy and regulation of key target genes during T-cell stimulation. *Nature*. 2007;445(7130):931-935. <https://doi.org/10.1038/nature05478>
  30. Josefowicz SZ, Lu L-F, Rudensky AY. Regulatory T cells: mechanisms of differentiation and function. *Annu Rev Immunol*. 2012;30(1):531-564. <https://doi.org/10.1146/annurev.immunol.25.022106.141623>
  31. Condeelis J, Pollard JW. Macrophages: obligate partners for tumor cell migration, invasion, and metastasis. *Cell*. 2006;124(2):263-266. <https://doi.org/10.1016/j.cell.2006.01.007>
  32. Greaves P, Clear A, Coutinho R, et al. Expression of FOXP3, CD68, and CD20 at diagnosis in the microenvironment of classical hodgkin lymphoma is predictive of outcome. *J Clin Oncol*. 2013;31(2):256-262. <https://doi.org/10.1200/jco.2011.39.9881>
  33. Diskin B, Adam S, Cassini M, et al. PD-L1 engagement on T cells promotes self-tolerance and suppression of neighboring macrophages and effector T cells in cancer. *Nat Immunol*. 2020;21(4):442-454. <https://doi.org/10.1038/s41590-020-0620-x>
  34. Agostinelli C, Gallamini A, Stracqualursi L, et al. The combined role of biomarkers and interim PET scan in prediction of treatment outcome in classical Hodgkin's lymphoma: a retrospective, European, multi-centre cohort study. *Lancet Haematol*. 2016;3(10):e467-e479. [https://doi.org/10.1016/s2352-3026\(16\)30108-9](https://doi.org/10.1016/s2352-3026(16)30108-9)
  35. Hiam-Galvez KJ, Allen BM, Spitzer MH. Systemic immunity in cancer. *Nat Rev Cancer*. 2021;21(6):345-359. <https://doi.org/10.1038/s41568-021-00347-z>
  36. de Charette M, Houot R. Hide or defend, the two strategies of lymphoma immune evasion: potential implications for immunotherapy. *Haematologica*. 2018;103(8):1256-1268. <https://doi.org/10.3324/haematol.2017.184192>
  37. Kanoun S, Berriolo-Riedinger A, Cottreau AS, et al. Total metabolic tumor volume and tumor dissemination are independent prognostic factors in advanced hodgkin lymphoma. *Blood*. 2021;138(Suppl 1):880. <https://doi.org/10.1182/blood-2021-147177>
  38. Cottreau AS, Versari A, Loft A, et al. Prognostic value of baseline metabolic tumor volume in early-stage Hodgkin lymphoma in the standard arm of the H10 trial. *Blood*. 2018;131(13):1456-1463. <https://doi.org/10.1182/blood-2017-07-795476>

## SUPPORTING INFORMATION

Additional supporting information can be found online in the Supporting Information section at the end of this article.

**How to cite this article:** Durmo R, Donati B, Rebaud L, et al. Prognostic value of lesion dissemination in doxorubicin, bleomycin, vinblastine, and dacarbazine-treated, interimPET-negative classical Hodgkin Lymphoma patients: A radio-genomic study. *Hematol Oncol*. 2022;40(4):645-657. <https://doi.org/10.1002/hon.3025>